Microchip laser operation of Tm,Ho:KLu(WO_4)$_2$ crystal

Pavel Loiko,[1,2] Josep Maria Serres,[2] Xavier Mateos,[2,*] Konstantin Yumashev,[1] Nikolai Kuleshov,[1] Valentin Petrov,[3] Uwe Griebner,[3] Magdalena Aguiló,[2] and Francesc Díaz[2]

[1]*Center for Optical Materials and Technologies, Belarusian National Technical University, 65/17 Nezavisimosti Ave., 220013 Minsk, Belarus*

[2]*Física i Cristal·lografia de Materials i Nanomaterials (FiCMA-FiCNA), Universitat Rovira i Virgili (URV), Campus Sescelades, c/ Marcel·lí Domingo, s/n., Tarragona, E-43007 Spain*

[3]*Max Born Institute for Nonlinear Optics and Short Pulse Spectroscopy, 2A Max-Born-Str., Berlin, D-12489 Germany*

[*]*xavier.mateos@urv.cat*

Abstract: A microchip laser is realized on the basis of a monoclinic Tm,Ho-codoped KLu(WO_4)$_2$ crystal cut for light propagation along the N_g optical indicatrix axis. This crystal cut provides positive thermal lens with extremely weak astigmatism, S/M = 4%. High sensitivity factors, M = dD/dP_{abs}, of 24.9 and 24.1 m^{-1}/W for the *mg*- and *pg*- tangential planes are calculated with respect to the absorbed pump power. Such thermo-optic behavior is responsible for mode stabilization in the plano-plano microchip laser cavity, as well as the demonstrated perfect circular beam profile (M^2 < 1.1). Maximum continuous-wave output power of 450 mW is obtained with a slope efficiency of 31%. A set of output couplers is employed to achieve lasing in the spectral range of 2060-2096 nm. The increase of output coupler transmission results in deterioration of the laser performance attributed to the increased up-conversion losses.

OCIS codes: (140.3380) Laser materials; (140.6810) Thermal effects; (140.3480) Lasers, diode-pumped.

References and links

1. K. Scholle, S. Lamrini, P. Koopmann, and P. Fuhrberg, "2 μm laser sources and their possible applications," in *Frontiers in Guided Wave Optics and Optoelectronics*, B. Pal, ed. (Intech, 2010), pp. 471–500.
2. V. Petrov, M. C. Pujol, X. Mateos, O. Silvestre, S. Rivier, M. Aguilo, R. Sole, J. Liu, U. Griebner, and F. Diaz, "Growth and properties of KLu(WO_4)$_2$,and novel ytterbium and thulium lasers based on this monoclinic crystalline host," Laser Photon. Rev. **1**(2), 179–212 (2007).
3. V. Jambunathan, X. Mateos, M. C. Pujol, J. J. Carvajal, C. Zaldo, U. Griebner, V. Petrov, M. Aguiló, and F. Díaz, "Crystal growth, optical spectroscopy, and continuous-wave laser operation of Ho:KLu(WO_4)$_2$ crystals," Appl. Phys. B **116**(2), 455–466 (2014).
4. A. A. Lagatsky, F. Fusari, S. V. Kurilchik, V. E. Kisel, A. S. Yasukevich, N. V. Kuleshov, A. A. Pavlyuk, C. T. A. Brown, and W. Sibbett, "Optical spectroscopy and efficient continuous-wave operation near 2 μm for a Tm,Ho:KYW laser crystal," Appl. Phys. B **97**(2), 321–326 (2009).
5. A. A. Lagatsky, F. Fusari, S. Calvez, J. A. Gupta, V. E. Kisel, N. V. Kuleshov, C. T. A. Brown, M. D. Dawson, and W. Sibbett, "Passive mode locking of a Tm,Ho:KY(WO_4)$_2$ laser around 2 microm," Opt. Lett. **34**(17), 2587–2589 (2009).
6. A. A. Lagatsky, F. Fusari, S. Calvez, S. V. Kurilchik, V. E. Kisel, N. V. Kuleshov, M. D. Dawson, C. T. A. Brown, and W. Sibbett, "Femtosecond pulse operation of a Tm,Ho-codoped crystalline laser near 2 microm," Opt. Lett. **35**(2), 172–174 (2010).
7. V. Jambunathan, A. Schmidt, X. Mateos, M. C. Pujol, J. J. Carvajal, M. Aguiló, F. Díaz, U. Griebner, and V. Petrov, "Continuous-wave co-lasing in a monoclinic co-doped (Ho,Tm): KLu(WO_4)$_2$ crystal," Laser Phys. Lett. **8**(11), 799–803 (2011).
8. V. Jambunathan, A. Schmidt, X. Mateos, M. C. Pujol, U. Griebner, V. Petrov, C. Zaldo, M. Aguiló, and F. Díaz, "Crystal growth, optical spectroscopy and continuous-wave laser operation of co-doped (Ho,Tm):KLu(WO_4)$_2$ monoclinic crystals," J. Opt. Soc. Am. B **31**(7), 1415–1421 (2014).
9. V. Jambunathan, X. Mateos, M. C. Pujol, J. J. Carvajal, U. Griebner, V. Petrov, M. Aguiló, and F. Díaz, "Diode-pumped continuous-wave laser operation of co-doped (Ho,Tm):KLu(WO_4)$_2$ monoclinic crystal," Opt. Laser Technol. **54**, 326–328 (2013).

#220723 - $15.00 USD Received 11 Aug 2014; revised 25 Sep 2014; accepted 28 Sep 2014; published 4 Nov 2014

10. X. Mateos, F. Di Trapani, M. Aguiló, F. Díaz, U. Griebner, and V. Petrov, "Diode-pumped continuous-wave (Ho,Tm):KLu(WO_4)$_2$ laser with >1 W output power," Opt. Mater. Express, in press (2014).
11. V. Aleksandrov, A. Gluth, V. Petrov, I. Buchvarov, S. Y. Choi, M. H. Kim, F. Rotermund, X. Mateos, F. Díaz, and U. Griebner, "Tm,Ho:KLu(WO_4)$_2$ laser mode-locked near 2μm by single-walled carbon nanotubes," Opt. Express, in press (2014).
12. G. L. Bourdet and G. Lescroart, "Theoretical modeling and design of a Tm, Ho:$YLiF_4$ microchip laser," Appl. Opt. **38**(15), 3275–3281 (1999).
13. G. L. Bourdet and R. A. Muller, "Tm,Ho:YLF microchip laser under Ti:sapphire and diode pumping," Appl. Phys. B **70**(3), 345–349 (2000).
14. J. Izawa, H. Nakajima, H. Hara, and Y. Arimoto, "A tunable and longitudinal mode oscillation of a Tm,Ho:YLF microchip laser using an external etalon," Opt. Commun. **180**(1–3), 137–140 (2000).
15. B. Q. Yao, F. Chen, P. B. Meng, C. H. Zhang, and Y. Z. Wang, "Diode pumped operation of Tm,Ho:YAP microchip laser," Laser Phys. **21**(4), 674–676 (2011).
16. Z. G. Wang, B. Q. Yao, G. Li, Y. L. Ju, and Y. Z. Wang, "Single longitudinal mode lasing of Tm,Ho:YAP microchip laser at 2000.4 nm," Laser Phys. **20**(2), 458–461 (2010).
17. B. Q. Yao, F. Chen, C. T. Wu, Q. Wang, G. Li, C. H. Zhang, Y. Z. Wang, and Y. L. Ju, "Diode-end-pumped Tm,Ho:YVO_4 microchip laser at room temperature," Laser Phys. **21**(4), 663–666 (2011).
18. R. L. Zhou, Y. L. Ju, C. T. Wu, Z. G. Wang, and Y. Z. Wang, "A single-longitudinal-mode CW 0.25 mm Tm,Ho:$GdVO_4$ microchip laser," Laser Phys. **20**(6), 1320–1323 (2010).
19. P. A. Loiko, K. V. Yumashev, N. V. Kuleshov, V. G. Savitski, S. Calvez, D. Burns, and A. A. Pavlyuk, "Thermal lens study in diode pumped N_g- and N_p-cut Nd:KGd(WO_4)$_2$ laser crystals," Opt. Express **17**(26), 23536–23543 (2009).
20. M. S. Gaponenko, P. A. Loiko, N. V. Gusakova, K. V. Yumashev, N. V. Kuleshov, and A. A. Pavlyuk, "Thermal lensing and microchip laser performance of N_g-cut Tm^{3+}:KY(WO_4)$_2$ crystal," Appl. Phys. B **108**(3), 603–607 (2012).
21. P. A. Loiko, J. M. Serres, X. Mateos, K. V. Yumashev, N. V. Kuleshov, V. Petrov, U. Griebner, M. Aguiló, and F. Díaz, "Characterization of thermal lens in Tm:KLu(WO_4)$_2$ and microchip laser operation," Laser Phys. Lett. **11**(7), 075001 (2014).
22. J. M. Serres, X. Mateos, P. Loiko, K. Yumashev, N. Kuleshov, V. Petrov, U. Griebner, M. Aguiló, and F. Díaz, "Diode-pumped microchip Tm:KLu(WO_4)$_2$ laser with more than 3 W of output power," Opt. Lett. **39**(14), 4247–4250 (2014).
23. V. G. Savitski, R. B. Birch, E. Fraczek, A. J. Kemp, P. A. Loiko, K. V. Yumashev, N. V. Kuleshov, and A. A. Pavlyuk, "The prospects for Yb- and Nd-doped tungstate microchip lasers," in *CLEO/ Europe-EQEC 2013*, Munich, May, 12–16 (2013), p. CA-10.5.
24. P. A. Loiko, V. G. Savitski, A. Kemp, A. A. Pavlyuk, N. V. Kuleshov, and K. V. Yumashev, "Anisotropy of the photo-elastic effect in Nd:KGd(WO_4)$_2$ laser crystals," Laser Phys. Lett. **11**(5), 055002 (2014).
25. P. A. Loiko, S. M. Vatnik, I. A. Vedin, A. A. Pavlyuk, K. V. Yumashev, and N. V. Kuleshov, "Thermal lensing in N_m-cut monoclinic Tm:KLu(WO_4)$_2$ laser crystal," Laser Phys. Lett. **10**(12), 125005 (2013).
26. X. Zhang, Y. Wang, L. Li, Y. Ju, and Y. Peng, "The effects of energy transfer upconversion on end-pumped Q-switched Tm, Ho:YLF lasers," J. Phys. D Appl. Phys. **42**(2), 025107 (2009).

1. Introduction

The Holmium (Ho^{3+}) ion attracts attention due its wavelength-tunable emission around 2 μm ($^5I_7 \rightarrow {}^5I_8$ transition). Such emission is eye-safe and of practical interest for remote sensing (LIDAR technology), metrology and medical applications. Ho lasers are also used for pumping of mid-IR optical parametric oscillators (OPOs) [1]. In the latter application, Ho laser emission (slightly above 2 μm) is preferable against that of Tm^{3+} (slightly below 2 μm) to avoid two-photon absorption in non-oxide non-linear crystals. Tm,Ho codoping of a laser host material brings the feature of enhanced pump efficiency and the possibility to increase the output power because the strong absorption of Tm ions in the range of 795-802 nm matches the output of AlGaAs laser diodes and subsequent energy transfer, $^3F_4(Tm) \rightarrow {}^5I_7(Ho)$ results in the excitation of the upper laser level of Ho. In recent years, several hosts were studied for Tm,Ho codoping, like $LiYF_4$ (YLF), $YAlO_3$ (YAP), YVO_4, $GdVO_4$, etc., and efficient lasers were realized with such gain materials. The above mentioned applications require high pump power and high efficiency at 2 μm, attainable only by means of high power diode pumping of the active medium. Thus, the codoped Tm,Ho system seems to be a feasible approach to generate 2 μm coherent radiation at high pump power since diode technology to pump directly the upper laser level of Ho is not mature [1].

Monoclinic potassium (rare-earth) double tungstates (DTs), with chemical formula K*RE*(WO_4)$_2$, where *RE* denotes Gd, Y or Lu, are potential hosts for Tm and Ho doping, offering high dopant concentration with low concentration-quenching, as well as large and

#220723 - $15.00 USD Received 11 Aug 2014; revised 25 Sep 2014; accepted 28 Sep 2014; published 4 Nov 2014

broad polarized absorption and emission bands. $KLu(WO_4)_2$ or shortly KLuW, compared to its counterparts KGdW and KYW, provides better crystal quality with lower level of defects when doped with active ions of ionic radii close to that of the "passive" Lu, such as Tm [2] and Ho [3]. In recent years, a substantial progress was achieved in the field of Tm,Ho:DT lasers. Lagatsky et al. demonstrated continuous-wave (CW) laser operation of Ho in the isostructural Tm,Ho:KYW laser crystal pumping with a Ti:Sapphire laser and achieving 460 mW of output power [4]. Later on, this work was extended to ultrashort pulse generation in picosecond [5] and femtosecond [6] regimes achieving pulses of 570 fs duration at a wavelength of 2055 nm. As KLuW is more suitable for Tm,Ho-codoping, further research focused on this host. Using Ti:Sapphire laser pumping, dual-wavelength operation was initially observed, preventing the achievement of high output power. The laser wavelength corresponding to Ho was 2061 nm and that to Tm was 1937 nm [7]. This study was extended to other doping levels [8] but modest results in terms of output power and slope efficiency (145 mW and 12.9%, respectively) were achieved. Diode-pumping was also studied [9] but again the output power did not exceed 100 mW. Only recently, with improved mode-matching, the output power of the Ho laser under both Ti:Sapphire and diode-pumping was substantially increased reaching the watt-level at 2060 nm [10] with tuning covering 180 nm at the zero level. Picosecond pulse generation in Tm,Ho:KLuW laser was also reported [11].

So far, the potential of Tm,Ho:KLuW for compact microchip lasers has not been studied, as already done with other hosts. Most developed are the Tm,Ho:YLF microchip lasers. Indeed, ~1 W of CW output at 2068 nm with a slope efficiency of 54% was obtained from such a laser under Ti:Sapphire pumping [12]. Subsequently, diode-pumping was also studied [13], yielding ~300 mW of CW output with slightly reduced slope efficiency of 49%. The single longitudinal mode (SLM) regime was observed in [14]. A diode-pumped Tm,Ho:YAP microchip allowed for the generation of ~170 mW with a moderate slope of 6% which increased to 12% at 77 K [15]. SLM operation with Tm,Ho:YAP was also reported [16]. A Tm,Ho:YVO_4 microchip generated 47 mW in CW at 2052 nm with 9% slope efficiency [17]. Using a Tm,Ho:$GdVO_4$ crystal, ~180 mW were obtained with a slope efficiency of 23% [18]. The SLM regime was realized with both vanadates.

For Tm,Ho:KLuW, the main challenge comes from the requirement of mode stabilization in a plano-plano cavity with a microchip set-up. DTs are typically cut along the growth direction, or *b*-axis || N_p-axis of the optical indicatrix, generating a negative thermal lens that leads to the cavity instability [19]. Only recently it was shown that another cut, along N_g-axis, can provide the desired mode stabilization and Tm:DTs microchip lasers were developed [20,21]. Later on, the potential for power scaling to multi-watt levels was confirmed [22]. The feasibility of the N_g-cut Yb- and Nd-doped DTs for microchip lasers was also shown [23]. The present paper is devoted to the realization of the first Tm,Ho:KLuW microchip laser. A detailed experimental study of thermo-optic effects is presented which is crucial for the understanding of the thermal mechanism of mode stabilization. As a result, we achieve the highest output power among all reported Tm,Ho-codoped diode-pumped microchip lasers.

2. Experimental

The studied crystal had the composition of 5at.% Tm, 0.5at.% Ho:KLuW. It was grown by the Top-Seeded Solution Growth (TSSG) slow-cooling method [2]. The starting materials were K_2CO_3, WO_3, and Ln_2O_3 (*Ln* = Lu, Tm and Ho) with 99.99% purity. The seed was oriented along the ***b*** crystallographic direction being perpendicular to the solution. From the as-grown bulk, two rectangular crystalline samples were cut perpendicular to the optical indicatrix axes, N_p, N_m and N_g, having the dimensions of 2.86(*g*) × 2.86(*m*) × 2.94(*p*) mm^3 and 1.50(*g*) × 3.05(*m*) × 3.01(*p*) mm^3. Both uncoated crystalline samples were tested for light propagation along the N_g axis (this crystal orientation is denoted as N_g-cut), the input and output crystal faces ($N_m \times N_p$) were polished to laser quality.

For the thermal lens measurements, the 2.86 mm-thick crystal was used. It was mounted in a water-cooled copper holder (kept at 14 °C) that provided cooling to all four lateral faces of the sample. Indium foil was used to improve the thermal contact. The crystal was placed into

#220723 - $15.00 USD Received 11 Aug 2014; revised 25 Sep 2014; accepted 28 Sep 2014; published 4 Nov 2014

a hemispherical laser cavity, Fig. 1(a). The flat pump mirror, PM, was antireflection (AR) coated from 770 to 1050 nm, and high-reflection (HR, R >99.9%) coated for 1820-2075 nm. The concave output coupler (OC) with radius of curvature of 50 mm, had a transmittance, T_{OC} = 3%, for the range 1820-2075 nm. The crystal was positioned close to the PM, with a separation of 1 mm. The overall cavity length was ~49 mm. The crystal was pumped by a fiber-coupler laser diode (NA = 0.22, fiber core diameter: 200 μm) operating at ~805 nm (pump of the $^3H_6 \rightarrow {}^3H_4$ transition of Tm^{3+}). The output of the diode was reimaged into the crystal by a lens assembly with 1:1 image ratio (pump spot radius: 100 μm). The absorption of the pump radiation was 60% and 47% for the two crystals with thickness of 2.86 mm and 1.50 mm, respectively. It was almost independent of the pump level and no absorption bleaching was observed. The parameters of the thermal lens were determined from the thermally-induced spatial distortions of the output laser beam [24]. To observe such distortions, we measured the beam diameter versus absorbed pump power P_{abs} for two principal meridional planes, namely the *mg*- and *pg*-plane, at 13 cm from the OC, with an optical knife-edge. The optical power of the thermal lens D was determined with the ABCD method.

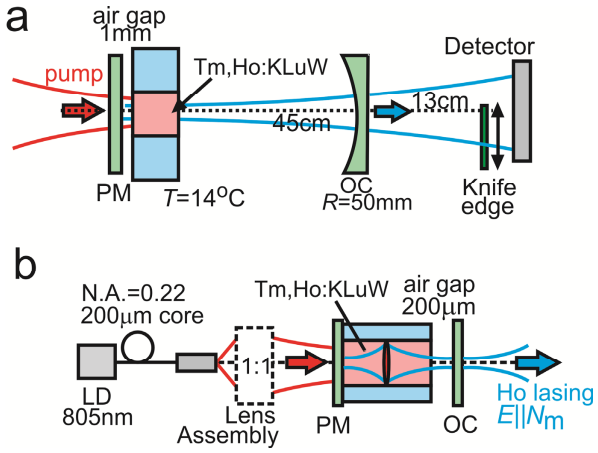

Fig. 1. Setups of the Tm,Ho:KLuW lasers investigated. (a) Hemispherical cavity for thermal lens measurements. (b) Microchip laser cavity. (PM: pump mirror, OC: output coupler, LD: laser diode).

Microchip laser operation of Tm,Ho:KLuW was studied in a plano-plano cavity, Fig. 1(b). In order to ensure validity of the previously determined parameters of the thermal lens for the description of mode stabilization in a microchip cavity, we used the same 2.86 mm-thick crystal, cooling and pumping systems as described above. The laser cavity was formed by a flat PM (AR-coated for ~805 nm, HR-coated for 1820-2075 nm) attached directly to the input face of the crystal and a flat OC separated from the crystal surface by a ~200 μm air gap. Five OCs with measured transmittance of 0.2% at 2081-2096 nm, 2.1% at 2080 nm, 3.1%, 5.1% or 9.1% at 2060 nm were studied (the wavelengths denoted correspond exactly to the laser emission experimentally observed). We also studied the shorter (1.50 mm-thick) Tm,Ho: KLuW crystal in the same microchip cavity with a thinner cooling holder (again in contact with all 4 sides) in order to realize more uniform heat deposition. All lasers described operated in the CW mode.

3. Results and discussion

The emission of the Tm,Ho:KLuW laser used for thermal lens measurements [Fig. 1(a)] was linearly polarized ($\boldsymbol{E} \parallel N_m$) emitting at ~2063 nm. The measured diameters of the output beam for the *mg*- and *pg*-planes are plotted in Fig. 2(a) as symbols. They clearly decrease with pump power. In accordance with the ABCD modeling, the decreased diameter corresponds to a positive thermal lens represented by the curves in Fig. 2(a). The observed focusing thermal

#220723 - $15.00 USD Received 11 Aug 2014; revised 25 Sep 2014; accepted 28 Sep 2014; published 4 Nov 2014

lens results in a stronger beam confinement, schematically depicted in the inset of Fig. 2(a). The calculated values of the optical power D are shown in Fig. 2(b) as symbols, together with their linear fittings. The latter yield the so-called sensitivity factor of the thermal lens, $M = dD/dP_{abs}$, which amounts to + 24.9 and + 24.1 m^{-1}/W for the *mg*- and *pg*- meridional planes, respectively. Thus, one can conclude that the thermal lens is purely positive (for any meridional plane). The difference $S = M_{mg} - M_{pg} = 0.8$ m^{-1}/W is called astigmatism degree which is responsible for the ellipticity of the laser beam. In the case of N_g-cut Tm,Ho:KLuW, it is rather small hence the thermal lens is close to spherical. Indeed, if expressed as S/M_{mg}, it equals only 4%.

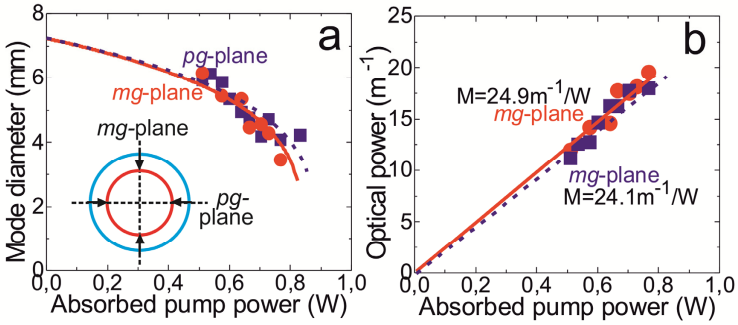

Fig. 2. Laser characteristics of Tm,Ho:KLuW in the hemispherical laser cavity (position: 13 cm away from the OC). (a) Mode diameter of the output beam *vs*. absorbed pump power, *symbols*: experimental data, *curves*: data fitting using the ABCD method, *inset:* scheme representing the distortion of the output laser beam profile (*blue circle* – near the threshold, *red circle* – at a high pump level). (b) Calculated optical power of the thermal lens (*symbols*) and the corresponding linear fits.

The thermo-optic properties of Tm,Ho:KLuW are summarized in Table 1, together with recent data for singly Tm-doped KLuW [21]. The crystal cut is along the N_g-axis (light polarization $\boldsymbol{E} \parallel N_m$).

Table 1. Thermo-optic Characterization of Diode-pumped N_g-cut Tm-doped [21] and Tm,Ho-codoped KLuW Crystals*

Crystal	λ, nm	M-factor, m^{-1}/W	S, m^{-1}/W^{-1}	S/M, %
Tm:KLuW	1951	+ 12.9 (*pg*), + 8.1 (*mg*)	4.8	37
Tm,Ho:KLuW	2061	+ 24.1 (*pg*), + 24.9 (*mg*)	0.8	4
Crystal	dn/dT, 10^{-6} K^{-1}	P_{PE}, 10^{-6} K^{-1}	Q_{dist}, 10^{-6} K^{-1}	χ, 10^{-6} K^{-1}
Tm:KLuW	–5.9	+ 1.7 (*pg*), –1.6 (*mg*)	+ 13.0	+ 8.8 (*pg*), + 5.5 (*mg*)
Tm,Ho:KLuW	–6.0	+ 2.1 (*pg*), + 2.4 (*mg*)	+ 13.0	+ 9.1 (*pg*), + 9.4 (*mg*)

*M - thermal lens sensitivity factor; S - astigmatism degree; P_{PE} – photoelestic effect; Q_{dist} – microscopic bulging; χ – "generalized" thermo-optic coefficient. The principal meridional planes are denoted in brackets.

From Table 1, it is clear that Tm,Ho-codoped KLuW generates a nearly two times stronger thermal lens as compared with singly Tm-doped KLuW. This is related to the different heat dissipation that can be expressed by a fractional heat loading, η_h. For a Tm-doped crystal, pumping at ~800 nm leads to excitation of Tm ions into the $^3H_4$ state, see Fig. 3. The resulting population of the lower-lying $^3F_4$ excited state is decreased due to the highly efficient two-for-one cross-relaxation scheme that reduces the heat release. Indeed, for Tm:KLuW, η_h was measured to be only ~0.25 ± 0.05 [25]. For a Tm,Ho-codoped crystal, a fraction of the energy stored in the $^3F_4$ manifold of Tm is transferred to the $^5I_7$ state of Ho. As a consequence the main source of heat release are energy-transfer up-conversion processes,

#220723 - $15.00 USD Received 11 Aug 2014; revised 25 Sep 2014; accepted 28 Sep 2014; published 4 Nov 2014

like $^3F_4$(Tm) + $^5I_7$(Ho) $\rightarrow$$^3H_6$(Tm) + $^5I_5$(Ho), followed by multiphonon relaxation from the higher-lying $^5I_5$ state. For another Tm,Ho-codoped host, YLF, η_h reaches ~0.45 ± 0.05 [26], a factor of ~1.8 larger. This is in clear agreement with the ~1.8 ratio of *M*-factors for Tm,Ho:KLuW and Tm:KLuW.

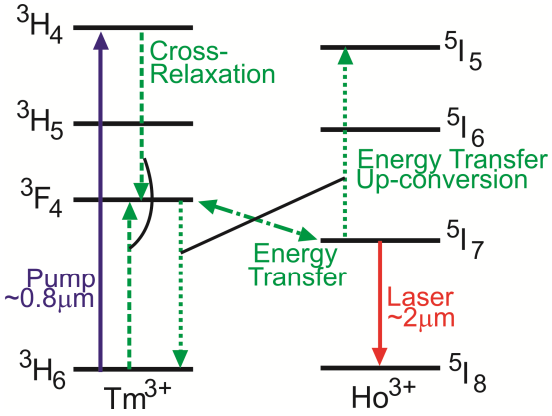

Fig. 3. Energy levels diagram of the Tm,Ho system with the energy levels involved in the absorption, cross-relaxation, energy transfer, up-conversion and laser generation around 2 μm processes.

In Table 1, we also extract the main contributions to the change of the optical path length for a diode-pumped crystal, i.e. temperature-induced variation of the refractive index (expressed by the thermo-optic coefficient d*n*/d*T*), the photoelastic effect (P_{PE} term) and microscopic crystal bulging due to axial strain (Q_{dist} term). The sum of these terms is called "generalized" thermo-optic coefficient, χ. The value of χ refers to the material parameters only, so it is inherent for the chosen laser crystal. There is a direct relation between sensitivity factor of the thermal lens *M* and χ value [24]:

$$M = \frac{\eta_h}{2\pi w_p^2 \kappa}\left(\frac{dn}{dT} + P_{PE} + Q_{dist}\right), \qquad (1)$$

where η_h is the above-mentioned fractional heat loading, w_p is the pump spot radius ("top-hat" beam profile) and κ is the thermal conductivity averaged over the plane of predominant heat removal (i.e. the plane perpendicular to the direction of propagation). The details of such a calculation can be found elsewhere [24]. From Table 1, one can conclude that the near-spherical and purely positive thermal lens in N_g-cut Tm,Ho:KLuW crystal is due to the dominant positive effect of axial strain (thermal expansion) over negative d*n*/d*T*, as well as vanishing impact of the photoelastic effect (P_{PE} ~2×10^{-6} K^{-1}). As a result, a kind of athermal thermo-optic behavior is observed. Another feature is the reduction of astigmatism for Tm,Ho:KLuW, *S*/*M* = 4%, compared with 37% for Tm:KLuW. This can be explained, taking into account that the astigmatism of the thermal lens is primarily determined by the anisotropy of the photoelastic effect (i.e. difference between the P_{PE} terms) that is much stronger for single Tm-doped crystal as compared with Tm,Ho-codoped one (as can be concluded from Table 1). The value of P_{PE} is dependent on the so-called elastic and photoelastic constants that vary with the crystal doping. Partially, the above mentioned effect can be associated with the particular cooling geometry.

The determined properties of the thermal lens in Tm,Ho:KLuW enables the desired mode stabilization in the plano-plano microchip laser cavity. The "standard" cut along the growth direction, $\boldsymbol{b} \parallel N_p$, would lead to an unstable behaviour due to the negative thermal lens. Indeed, laser operation in the microchip set-up depicted in Fig. 1(b) was obtained for all studied T_{OC} and the laser output was always linearly polarized ($\boldsymbol{E} \parallel N_m$). The polarization was naturally-selected by the anisotropy of the gain. The input-output dependences for the 2.86

#220723 - $15.00 USD Received 11 Aug 2014; revised 25 Sep 2014; accepted 28 Sep 2014; published 4 Nov 2014

mm-thick crystal are presented in Fig. 4(a). The main laser characteristics (slope efficiency η, optical-to-optical efficiency η_{opt}, highest achieved output power P_{out} and laser wavelength λ_l) are also summarized in Table 2. Laser oscillation started at 0.5 W of absorbed pump power and the maximum output power amounted to 451 mW (P_{abs} = 2.8 W). The corresponding slope efficiency was 31% and the optical-to-optical efficiency 16%, achieved for T_{OC} = 2.1% when considering the range with linear dependence of the output power with absorbed pump power as shown in Fig. 4(a).

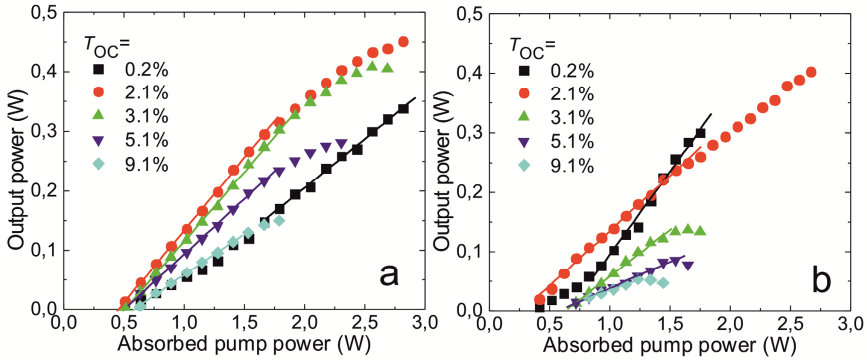

Fig. 4. CW output power *vs*. absorbed pump power for the Tm,Ho:KLuW microchip lasers. The crystal thickness is 2.86 mm (a) and 1.50 mm (b).

Table 2. Output Characteristics of the Tm,Ho:KLuW Microchip Laser for Different T_{OC} (Crystal Thickness: 2.86 mm)*

T_{OC}	P_{out}, mW	λ_l, nm	η, %	η_{opt}, %
0.2%	338	2081-096	17	12
2.1%	451	2081	31	16
3.1%	408	2063	30	16
5.1%	281	2061	22	12
9.1%	150	2061	12	8

*P_{out} - maximum output power; λ_l - laser wavelength; η- slope efficiency; η_{opt} - optical-to-optical efficiency

With the increase of T_{OC}, the output power and slope efficiency of the Tm,Ho:KLuW microchip laser decreases. Moreover, at some critical value of P_{abs}, the output power begins to decrease. All the measurements presented in Fig. 4(a) were performed up to this point in order to avoid crystal damage. For maximum T_{OC} = 9.1%, nearly three-times lower output characteristics are observed as compared with T_{OC} = 2.1%, namely P_{out} = 150 mW and η = 12%. We attribute this behavior to an increase of up-conversion losses because laser operation with higher T_{OC} requires a higher inversion ratio β which means higher population of the upper-laser level of Ho^{3+} ions. This, in turn, means higher probability for transitions from the upper-laser level to upper-lying excited states involved in up-conversion processes. The inversion ratio, β is the ratio of the excited ions to the total ion density. It is defined as $\beta = N_2/N$ and $N_1 = (1-\beta)N$, with the total ion density $N = N_1 + N_2$.

In order to verify this explanation, we also tested the thinner (1.50 mm) Tm,Ho:KLuW crystal in the same microchip laser set-up, Fig. 1(b). It ensured a more uniform distribution of heat loading due to the lower pump absorption. The output characteristics are presented in Fig. 4(b), and the tendency is in agreement with the 2.86 mm-thick crystal. The highest output power again corresponds to T_{OC} = 2.1% (403 mW at 2.7 W of absorbed pump power, slope efficiency η = 17% and optical-to-optical efficiency η_{opt} = 15%). The laser threshold is slightly reduced to 0.41 W due to lower reabsorption losses in the thinner crystal. The highest slope efficiency corresponds to T_{OC} = 0.2%, namely 28%. High OC transmittance results in poor laser performance. Thus, for T_{OC} = 9.1%, P_{out} = 55 mW and η = 7% was achieved. Note that for a given T_{OC} the inversion ratio β is in general higher for the thinner crystal because the doping level is the same and the overall performance in Figs. 4(a) and 4(b) is different.

#220723 - $15.00 USD Received 11 Aug 2014; revised 25 Sep 2014; accepted 28 Sep 2014; published 4 Nov 2014

The increase of T_{OC} also leads to a shift of λ_l to shorter wavelengths, see Fig. 5(a). This is a well-known effect for quasi-three level lasers where the gain spectrum depends on the inversion ratio β. In particular, for P_{abs} = 1.3 W and for T_{OC} = 3.1, 5.1 and 9.1%, laser oscillation occurred around 2061 nm and this was maintained for all the range of absorbed powers, corresponding to a local maximum in the gain spectrum of Ho in KLuW, see Fig. 5(c). In contrast, for T_{OC} = 2.1% the laser emitted at 2081 nm, matching a different local maximum which is more pronounced at lower β. At P_{abs} > 2 W [Fig. 5(b)] the laser wavelength shifted to 2060 nm due to the change in the inversion ratio caused by thermal effects, see Fig. 5(c), for increased absorbed power. Applying T_{OC} = 0.2% lasing occurred in the range of 2081-2096 nm obviously corresponding to β < 0.22. The latter is characterized by a very smooth gain profile [Fig. 5(c)] explaining the few laser lines observed.

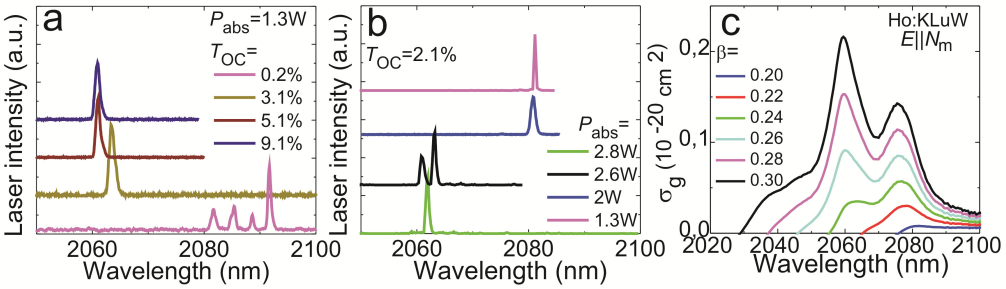

Fig. 5. Evolution of the laser spectrum of the Tm,Ho:KLuW microchip laser (crystal thickness: 2.86 mm) with the change of output coupling, T_{OC} at an absorbed pump power of P_{abs} = 1.3W, (a) and absorbed pump power, P_{abs} for T_{OC} = 2.1% (b). Gain cross-section, σ_g of Ho in KLuW for different inversion rates β, (light polarization: $\boldsymbol{E} \parallel N_m$) (c).

The output beam profile of the Tm,Ho:KLuW microchip laser recorded with a near-IR camera is shown in Fig. 6 (2.86 mm-thick crystal, 13 cm from OC, T_{OC} = 2.1%, P_{abs} = 2.7 W). As expected from the low astigmatism of the thermal lens (S/M = 4%), the beam is perfectly circular. Cuts through the profile for both the *mg*- and *pg*-plane, are also enclosed in Fig. 6 (symbols: experimental data, curves: Gaussian fits); The two cuts are slightly shifted for clarity. Both profiles are very close to Gaussian ones, meaning the laser oscillations occur at the TEM_{00} mode. In contrast to the hemispherical cavity, the thermal lens in the microchip set-up leads to slight beam expansion, as depicted in the inset in Fig. 6. The beam quality factor M^2 for the Tm,Ho:KLuW microchip laser was below 1.1.

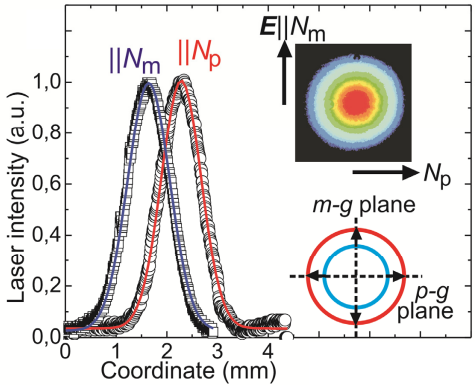

Fig. 6. Spatial beam profiles of the Tm,Ho:KLuW microchip laser along the N_p and N_m axes (*symbols*) and their Gaussian fits (*curves*), (position: 13 cm away from the OC; cuts are slightly shifted for better visibility), *insets* represent the image of the beam profile recorded with a near-IR camera and the schematic drawing of the beam deformation (*blue circle* – near the threshold, *red circle* – at a high pump level).

#220723 - $15.00 USD Received 11 Aug 2014; revised 25 Sep 2014; accepted 28 Sep 2014; published 4 Nov 2014

The reported results for the diode-pumped Tm,Ho:KLuW microchip laser are superior compared to all previous demonstrations with diode-pumped Tm,Ho-codoped YAP [15], YVO_4 or $GdVO_4$ [17,18], both in terms of output power and slope efficiency. In comparison with the state-of-the-art for Tm,Ho:YLF [13], we achieved 1.5-times increase of the output power. Further power scaling of the Tm,Ho:KLuW microchip laser can be realized with (i) optimization of output coupling between 0.2 and 2.1% to minimize up-conversion losses; (ii) appropriate selection of Tm/Ho ratio leading to higher energy transfer efficiency and lower up-conversion and reabsorption losses; (iii) improvement of the mode-matching.

4. Conclusions

Microchip laser operation of Tm,Ho:KLuW crystal is demonstrated for the first time to our knowledge. The presented results surpass all previous reported diode-pumped Tm,Ho-codoped microchip lasers with repect to the output power performance [12–18]. The laser generates 451 mW of CW output power at 2081 nm with a maximum slope efficiency of 31% (optical-to-optical efficiency of 16%). The laser performance is strongly dependent on the output coupling, most probably due to up-conversion losses; T_{OC} = 2.1% is found to be close to optimal. The mode stabilization in a plano-plano cavity for a microchip configuration is ensured by a special crystal cut along the N_g optical indicatrix axis. For N_g-cut Tm,Ho:KLuW, the thermal lens is positive for both principal meridional planes (M_{pg} = 24.1 and M_{mg} = 24.9 m^{-1}/W for a pump spot radius of 100 μm). The extremely low astigmatism of the thermal lens, S/M = 4%, is related to the low anisotropy of the photoelastic effect. This defines perfectly circular profile of the output beam with an M^2 factor < 1.1.

Acknowledgments

This work was supported by the Spanish Government under project MAT2011-29255-C02-02, MAT2013-47395-C4-4-R and by the Generalitat de Catalunya under project 2014SGR1358.

#220723 - $15.00 USD Received 11 Aug 2014; revised 25 Sep 2014; accepted 28 Sep 2014; published 4 Nov 2014